 Bull. Chem. Soc. Jpn. Vol. 84, No. 12, 1347–1354 (2011)

Differences of Structures and Electronic Properties in the Triplet States between Dibromo and Dichloro Mononuclear Polypyridine Iridium(III) Complexes

Naokazu Yoshikawa,*[1] Shinichi Yamabe,[2] Nobuko Kanehisa,[3] Tsuyoshi Inoue,[3] Hiroshi Takashima,[1] and Keiichi Tsukahara[1]

[1]Department of Chemistry, Faculty of Science, Nara Women's University, Nara 630-8506

[2]Department of Chemistry, Nara University of Education, Nara 630-8528

[3]Department of Applied Chemistry, Graduate School of Engineering, Osaka University, Osaka 565-0871

Received April 6, 2011; E-mail: naokazuu@dream.com

Emission and electronic properties of eight iridium(III)-centered polypyridine complexes were studied systematically. A crystal structure of $[IrBr_2(phen)_2]PF_6$ was obtained by X-ray diffraction study, where phen is 1,10-phenanthroline. Those in the triplet states were also determined by DFT calculations to investigate the source of emission spectra. Two triplet structures of $[IrX_2(bpy)_2]^+$ and $[IrX_2(phen)_2]^+$ and the transition state of interconversion were obtained with $X^- = Cl^-$ and Br^-. Here, bpy is 2,2′-bipyridine. For the chloro complexes, two triplet species have nonequivalent bpy and phen ligands through pseudo-Jahn–Teller geometric distortion. The dichloro complexes with asymmetric spin density distributions were found to correspond to stronger emission spectra than those for the dibromo compounds. Energies (E_{em}'s) corresponding to the observed emission wavelengths (λ_{em}'s) are in good agreement with the theoretical S_0–T_1 energy differences (ΔE's). For $[IrBr_2(bpy)_2]^+$, $E_{em} = 2.29$ eV and $\Delta E = 2.26$ eV. For $[IrCl_2(bpy)_2]^+$, $E_{em} = 2.29$ eV and $\Delta E = 2.33$ eV. For $[IrBr_2(phen)_2]^+$, $E_{em} = 2.26$ eV and $\Delta E = 2.28$ eV. For $[IrCl_2(phen)_2]^+$, $E_{em} = 2.28$ eV and $\Delta E = 2.34$ eV. For all the four complexes, **1A**, **1B**, **3A**, and **3B**, DFT calculations indicate Ir–N bond rupture. T_c with a small S_0–T_1 energy-gap would undergo nonradiative relaxation. T_c indicates a triplet state which is a five-coordinate species with triplet metal-centered character. Coexistence of the triplet state species are discussed in terms of their electronic structures.

Polypyridine complexes of d^6 transition metals have been widely studied because of their useful spectroscopic and photophysical properties. Complexes of second-row and third-row transition metals with polypyridine ligands are particularly interesting, because they exhibit strong phosphorescence due to the mixing of singlet and triplet excited states via spin–orbit coupling. Recently, iridium(III) cyclometalated complexes have attracted much attention because of their possible applications to photonic devices[1–4] and LED displays.[5–9] In our previous work, we synthesized and crystallized the chloride containing complexes $[IrCl_2L_2]PF_6$ (L = 4,4′-dimethyl-2,2′-bipyridine, dipyridylpyrazine, and 2,2′-biquinoline), in order to examine their long-lived excited states and good photoluminescence efficiencies.[10] Recently, computational methods were used to predict or ensure photophysical properties of metal complexes.[11–15] Density functional theory (DFT) has been applied to studying the electronic effects of different ligands and substituents in the ground and excited states involved in the emission process. Time-dependent (TD) DFT calculations of the iridium cyclometalated complexes for OLED materials have been reported.[16–18]

In this work, the bromide containing complexes $[IrBr_2L_2]PF_6$ (L = 2,2′-bipyridine, 4,4′-dimethyl-2,2′-bipyridine, 1,10-phenanthroline, and 4,7-diphenyl-1,10-phenanthroline) have been newly prepared. A crystal structure of $[IrBr_2(phen)_2]PF_6$ has been obtained. There is spectroscopic interest in the differences in absorption, emission and lifetime observed between Cl complexes and Br complexes. We performed DFT calculations of four iridium(III) complexes **1A**, **3A**, **1B**, and **3B** with bidentate ligands and X = Cl and Br ligands along with the comparison of emission spectra of the eight complexes in Scheme 1. In particular, electronic structures of the triplet excited states of complexes were carefully examined. So far, there have been no DFT investigations of two electronic states in the iridium complexes and a transition state. Striking differences of the S_0–T_1 energy gaps and intensities of emission spectra were found.

Results and Discussion

Absorption Properties. Figure 1 shows the absorption spectra for the parent complexes **1A**, **1B**,[10] **3A**, and **3B**.[10] Absorption data of the eight complexes are shown in Table 1. For complex **1B**, UV absorption is found in the region of 247 nm, which is ascribable to intraligand centered (LC) transitions. At lower energies, an absorption shoulder is also found at 284 nm. For complexes **3A** and **3B**, peaks and shoulders at 337 and 392 nm are obtained and are shown in Figure 1. Almost the same absorption spectra are observed between complexes **1A** and **1B** and between complexes **3A** and **3B**. That is, they are nearly insensitive to the halide ion ($X^- = Cl^-$ or Br^-).

Published on the web December 6, 2011; doi:10.1246/bcsj.20110098

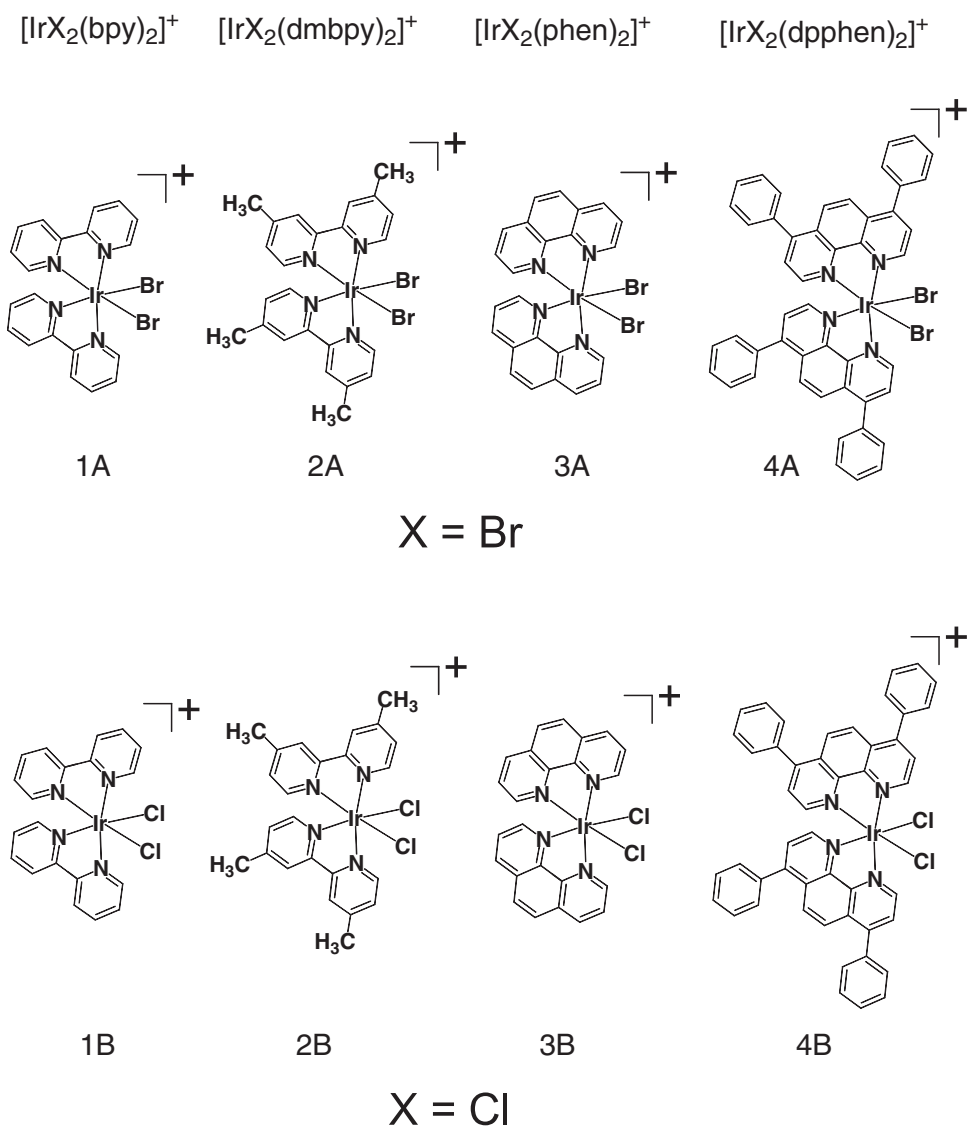

Scheme 1. Structural formulae of the iridium(III) complexes examined in this work.

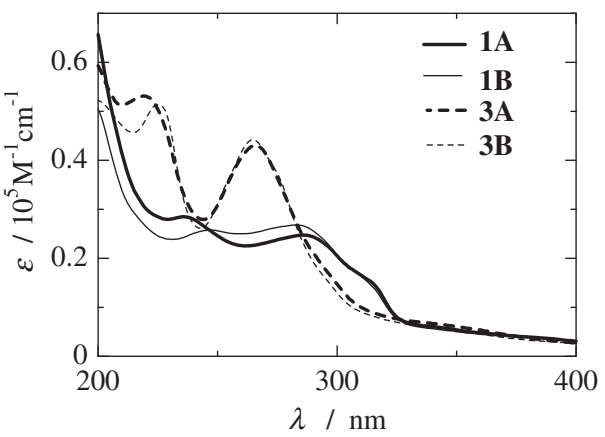

Figure 1. Electronic absorption spectra of the four substituent free complexes in CH_3CN solvent at room temperature.

Table 1. Electronic Absorption Spectral Properties of the Complexes in CH_3CN[a] Solvent

Complexes	λ_{max}/nm ($\varepsilon/10^4\,M^{-1}\,cm^{-1}$)
1A·PF_6^-	236 (2.45), 285 (2.21), 313 (1.54)[c]
2A·PF_6^-	236 (3.44), 274 (2.64), 307 (1.73)
3A·PF_6^-	219 (5.30), 266 (4.30), 337 (0.67)[c], 392 (0.30)[c]
4A·PF_6^-	219 (7.08), 283 (7.16), 327 (2.74)[c], 413 (0.62)[c]
1B·PF_6^-[b]	247 (2.57), 284 (2.67), 313 (1.54)[c]
2B·PF_6^-[b]	206 (5.33), 273 (2.53), 307 (1.60)
3B·PF_6^-[b]	225 (5.10), 265 (4.45), 337 (0.61)[c], 392 (0.30)
4B·PF_6^-[b]	219 (6.36), 282 (6.48), 327 (2.62), 413 (0.77)

a) UV–vis spectra of **1A**, **1B**, **3A**, and **3B** are shown in Figure 1. b) Ref. 10. c) Shoulder.

Table 2. Electrochemical Properties of the Complexes in CH_3CN

Cations	Complexes	E/V			
		Red 1st	Red 2nd	Red 3rd	Ox 1st
1A	$[IrBr_2(bpy)_2]PF_6$	−0.92	−1.19		1.78
2A	$[IrBr_2(dmbpy)_2]PF_6$	−1.16	−1.32		1.74
3A	$[IrBr_2(phen)_2]PF_6$	−1.18	−1.36		1.71
4A	$[IrBr_2(dpphen)_2]PF_6$	−1.04	−1.18		1.60
1B[a)]	$[IrCl_2(bpy)_2]PF_6$	−1.09	−1.28	−1.40	2.07
2B[a)]	$[IrCl_2(dmbpy)_2]PF_6$	−1.18	−1.34	−1.53	1.97
3B[a)]	$[IrCl_2(phen)_2]PF_6$	−1.07	−1.24	−1.47	2.05
4B[a)]	$[IrCl_2(dpphen)_2]PF_6$	−1.06	−1.22	−1.37	1.97

a) Ref. 10.

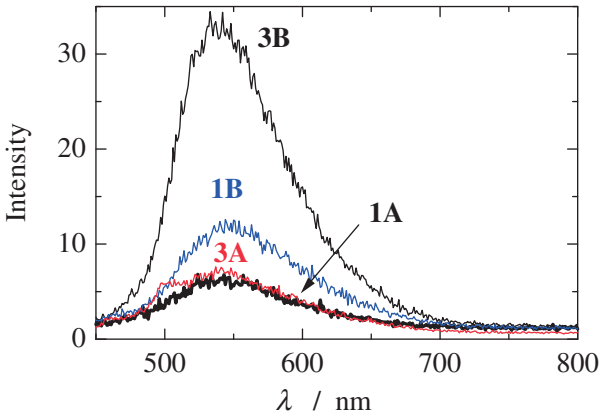

Figure 2. Emission spectra of the four complexes (1.00×10^{-5} M) in N_2-saturated CH_3CN at room temperature. The excitation wavelength λ_{ex} is 318 nm.

Table 3. Emission Properties of the Complexes in CH_3CN

Cation	Complexes	Emission				
		λ_{em}/nm (eV)[a)]	Φ[a)]	τ[b)]/ns	$k_r/10^6\,s^{-1}$ e)	$k_{nr}/10^6\,s^{-1}$ e)
1A	$[IrBr_2(bpy)_2]PF_6$	541 (2.292)	0.019	270	0.070	3.63
2A	$[IrBr_2(dmbpy)_2]PF_6$	560 (2.214)	0.009	240	0.038	4.13
3A	$[IrBr_2(phen)_2]PF_6$	548 (2.263)	0.028	290	0.097	3.35
4A	$[IrBr_2(dpphen)_2]PF_6$	561 (2.210)	0.047	740	0.064	1.29
1B	$[IrCl_2(bpy)_2]PF_6$	541 (2.292)	0.032	310[c)], 344[d)]	0.103	3.12
2B	$[IrCl_2(dmbpy)_2]PF_6$	532 (2.331)	0.059	300[c)]	0.197	3.14
3B	$[IrCl_2(phen)_2]PF_6$	542 (2.288)	0.14	720[c)]	0.194	1.19
4B	$[IrCl_2(dpphen)_2]PF_6$	551 (2.250)	0.057	1300[c)]	0.044	0.725

a) The emission quantum yields were determined at 298 K relative to those of a solution containing $[Ru(bpy)_3]^{2+}$ ($\Phi = 0.095$) and having the same absorbance. The excitation wavelength (λ_{ex}) = 318 nm. b) The emission lifetimes were measured in N_2-saturated CH_3CN solutions. λ_{ex} = 370 nm. c) Ref. 10. d) Ref. 19. e) The emission performance of the eight compounds was also studied by calculating the radiative (k_r) and nonradiative (k_{nr}) rate constants, which are defined as the Φ/τ and $(1-\Phi)/\tau$ ratios, respectively. Radiative (k_r) and nonradiative (k_{nr}) rate constants calculated from Φ and τ values; estimated uncertainty (20%).

Electrochemistry. The electrochemical properties of the dibromo(polypyridine)iridium(III) complexes were examined by differential pulse voltammetry in N_2-saturated CH_3CN at room temperature. Those of the dichloro complexes were reported in our previous work.[10] The redox potentials measured relative to an Ag/AgCl reference electrode are summarized in Table 2. For complex **1A**, an oxidation wave was observed at 1.78 V. This small oxidation potential relative to those of dichloro **B** series reflects the increase in the electronic density at the iridium center. An oxidation wave was also observed for the other complexes **2A** and **3A** at around 1.7 V. At negative potentials, complex **3A** exhibits a reversible one-electron process (Red 1st in Table 2) at −1.18 V. A similar pattern is observed for complex **4A** at −1.04 V. In comparison with the corresponding Cl^- complexes,[10] these processes can be assigned to the reduction of the phen and dpphen ligands, respectively. The LUMO can be assigned to the π^* orbital on the polypyridine ligands. A similar CV spectra was obtained between Cl^- complexes (**A** series) and Br^- complexes (**B** series).

Emission Properties. Figure 2 exhibits emission spectra of the four complexes, **1A**, **1B**, **3A**, and **3B**. The emission spectra of **1B**, **2B**, **3B**, and **4B** were reported previously.[10] Table 3 shows emission properties of eight complexes. Short lifetimes were obtained for the iridium complexes **1A**–**4A** [(**1A**, τ = 270 ns), (**2A**, τ = 240 ns), (**3A**, τ = 290 ns), and (**4A**, τ = 740 ns)] relative to those for complexes **1B**–**4B**. Intense emissions were observed in complexes **3B** and **4B** at room temperature. On the other hand, weak emission was obtained for Br iridium complexes **3A** and **4A**. The emission intensities are remarkably different in Figure 2.

Structural and Energetic Features. Ground-State Geometries of the Iridium Complexes: As a typical model, the coordination geometry of **3A** was scrutinized. The structure of **3A** was determined by X-ray crystallography, and the ORTEP of **3A** is given in Figure S1. The structure of $[IrBr_2(phen)_2]PF_6$ consists of a discrete $[IrBr_2(phen)_2]^+$ (**3A**) cation and a hexafluorophosphate anion PF_6^-. Crystallographic data of **3A** are shown in Table S1 (Supporting Information). Geometries of **1A**, **1B**, **3A**, and **3B** were optimized by DFT calculations by the use of the crystal structure of **3A** and are shown in Figure 3.

In order to investigate the source of the contrast between absorption and emission spectra, B3LYP calculations were carried out. Table 4 shows the obtained geometries of the triplet

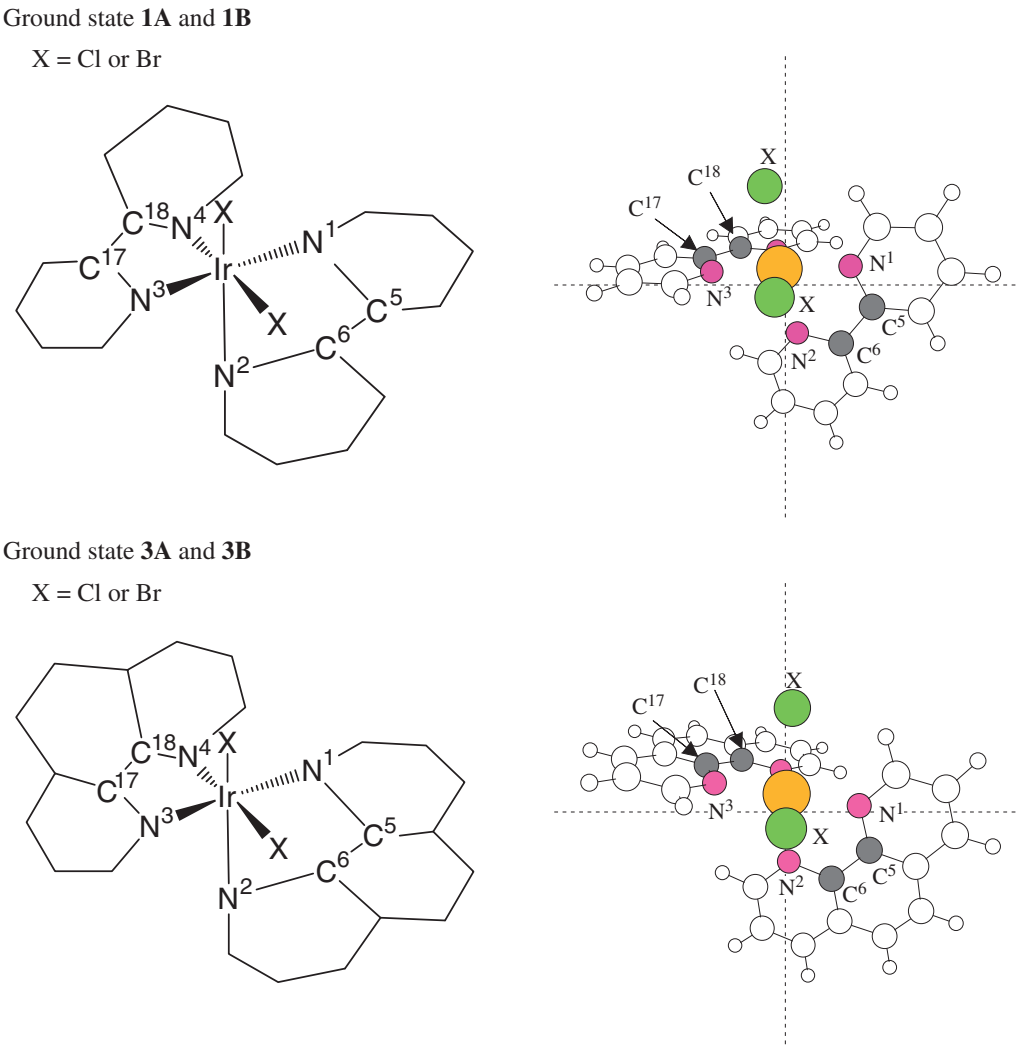

Figure 3. Geometries of ground states of $[IrBr_2(bpy)_2]^+$ (**1A**), $[IrCl_2(bpy)_2]^+$ (**1B**), $[IrBr_2(phen)_2]^+$ (**3A**), and $[IrCl_2(phen)_2]^+$ (**3B**). Main distances are in Table 4 and Cartesian coordinates are shown in Table S2 of Supporting Information.

states (T_a and T_c) of complex **1A** and (T_a, T_b, and T_c) complex **1B** along with those of the ground state (singlet). T_{ts} in Table 4 stands for the transition state for the $T_a \rightarrow T_b$ conversion. Cartesian coordinates of the ground state, T_a, T_{ts}, and T_b are in Table S2 of Supporting Information. The geometry of T_a was obtained by the use of the ground-state as the initial data. That of T_b was obtained by specifying the double bond (C5=C6) in one bpy ring in the initial geometric data. That of T_c was obtained by the initial geometry with the elongated N···Ir and Ir···X bonds in the line.

Between the complexes **1B** and **1A**, geometries of the ground state, T_a, and T_c are similar. The geometry of the triplet state T_a is close to that of singlet and T_a would be a vertically excited state. That of T_c is a five-coordinate species of the triplet metal-centered character. The distance of C5–C6 (=1.474 Å) is remarkably different from that of C17–C18 (=1.408 Å) for T_b of **1B**. The difference indicates that the two bpy rings are nonequivalent. On the other hand, they are equivalent (=1.44 Å) for T_a of **1B**. As a crucial difference, the T_b state is absent for the bromo series, **1A** and **3A**, but is present for the chloro complexes, **1B** and **3B**.

In Table 5, relative energy, ΔE is exhibited, ΔE is the difference of the sum of the electronic and zero-point vibrational energies between ground and triplet states and their positive values mean less stable systems. For complex **1B**, $E_{em} = 2.292$ eV (observed) is nearly the same as $\Delta E = +2.329$ eV of T_a and $\Delta E = +2.345$ eV of T_b (calculated). Thus, T_a and T_b are potentially emissive triplet spin states. The activation energy of T_{ts} for the interconversion is very small, and accordingly the state T_a would equilibrate with the state T_b. For complex **1A**, $E_{em} = 2.292$ eV is similar to $\Delta E = +2.256$ eV of T_a, but is larger than $\Delta E = +1.998$ eV of T_c.

Tables 4 and 5 also show the calculated geometries and energies of complexes **3B** and **3A**. They are similar to those of **1B** and **1A**, respectively. For complex **3B**, $\Delta E = 2.342$ eV (T_a) and $\Delta E = 2.363$ eV (T_b) are close to $E_{em} = 2.282$ eV. On the other hand, for complex **3A**, while $\Delta E = 2.278$ eV (T_a) is almost the same as $E_{em} = 2.263$ eV, $\Delta E = 1.967$ eV (T_c) is smaller than E_{em}. For the four complexes, **1A**, **1B**, **3A**, and **3B**, DFT calculations indicate bond rupture leading to a five-coordinate species that has triplet metal-centered character T_c small energy-gap of S_0–T_1.[20,21]

The triplet state is always split into three sub-states, at least if the symmetry of the molecule is sufficiently low. For a [Ir(ppy)$_3$], the total zero-field splitting energy has been determined to be 170 cm^{-1}.[21,22] Spin–orbit coupling carried by metal d-orbitals can drastically increase the magnitude of zero-field splitting.[23–26]

Figure 4 shows Mulliken spin densities of T_a and T_c of complex **1A**. While those of T_a are delocalized on Ir^{3+}, Br^-, and two bpy ligands, those of T_c are localized largely on Ir^{3+}, they are then subject to the heavy-atom effect and the consequent large spin–orbital interaction. The interaction would lead to nonradiative energy relaxation. Figure 5 exhibits spin densities of T_a, T_b, and T_c of complex **1B**. Those of T_a between **1A** (Figure 4) and **1B** (Figure 5) are similar. For T_b of complex **1B** (Figure 5), the densities are nearly missing in one bpy ligand, which corresponds to the geometric nonequivalence shown in Table 4. Spin densities of complexes **3A** and **3B** are shown in Figures S2 and S3, respectively. For the chloro complexes, **1B** and **3B**, two triplet species have

Table 4. Comparison of Calculated Bond Lengths and Dihedral Angles of the Ground State (Singlet) and the Triplet States (T_a, T_{ts}, T_b, and T_c) for Complexes **1A**, **1B**, **3A**, and **3B**[a)]

		Bond length/Å and dihedral angles/°				
		Ground state	T_a[b)]	T_{ts}[c)]	T_b[b)]	T_c[b)]
1A[a)]	Ir–N2	2.083	2.076			2.121
	Ir–N4	2.083	2.076			2.481
	Ir–Br1	2.539	2.486			2.699
	C5–C6	1.472	1.442			1.471
	C17–C18	1.472	1.442			1.482
	N3–C–C–N4	0.75	2.27			14.7
1B[a)]	Ir–N2	2.073	2.059	2.087	2.087	2.096
	Ir–N4	2.073	2.059	2.027	2.027	2.494
	Ir–Cl1	2.398	2.347	2.374	2.375	2.543
	C5–C6	1.472	1.441	1.474	1.474	1.471
	C17–C18	1.472	1.442	1.409	1.408	1.492
	N3–C–C–N4	1.21	1.5	0.5	0.5	16.46
3A[a)]	Ir–N2	2.094	2.075			2.139
	Ir–N4	2.094	2.075			2.501
	Ir–Br1	2.535	2.484			2.696
	C5–C6	1.426	1.408			1.425
	C17–C18	1.426	1.408			1.441
	N3–C–C–N4	0	1.77			1.42
3B[a)]	Ir–N2	2.083	2.066	2.092	2.102	2.125
	Ir–N4	2.083	2.059	2.036	2.020	2.494
	Ir–Cl1	2.394	2.346	2.364	2.380	2.564
	C5–C6	1.425	1.409	1.420	1.426	1.424
	C17–C18	1.425	1.406	1.396	1.390	1.440
	N3–C–C–N4	0.54	1.56	0.34	0.29	1.64

a) The atom numbering for **1A**, **1B**, **3A**, and **3B** is shown in Figure 3. b) T_a, T_b, and T_c are the structures of the triplet states. c) T_{ts} stands for the transition state for $T_a \rightarrow T_b$ conversion.

Table 5. Comparison of Relative Energies ΔE's, the Ground State (Singlet), and the Triplet States (T_a, T_{ts}, T_b, and T_c) for Complexes

Complexes	Relative energy ΔE[a)]/eV					E_{em}[b)]/eV
	Ground state	T_a	T_{ts}	T_b	T_c	exptl.
1A	0	2.256			1.998	2.292
	(0)	(2.376)			(2.053)	
1B	0	2.329	2.326	2.345	2.108	2.292
	(0)	(2.448)	(2.437)	(2.437)	(2.168)	
3A	0	2.278			1.967	2.263
	(0)	(2.406)			(2.026)	
3B	0	2.342	2.327	2.363	1.967	2.282
	(0)	(2.475)	(2.477)	(2.473)	(2.074)	

a) T_a, T_b, and T_c are the structures of the triplet states. T_{ts} stands for the transition state for $T_a \rightarrow T_b$ conversion. Those with the parentheses are differences of electronic energies, and those without ones are by sum of electronic and zero-point vibration energies. b) E_{em} is the energy which corresponds to the wavelength (λ_{em}) shown in Table 3.

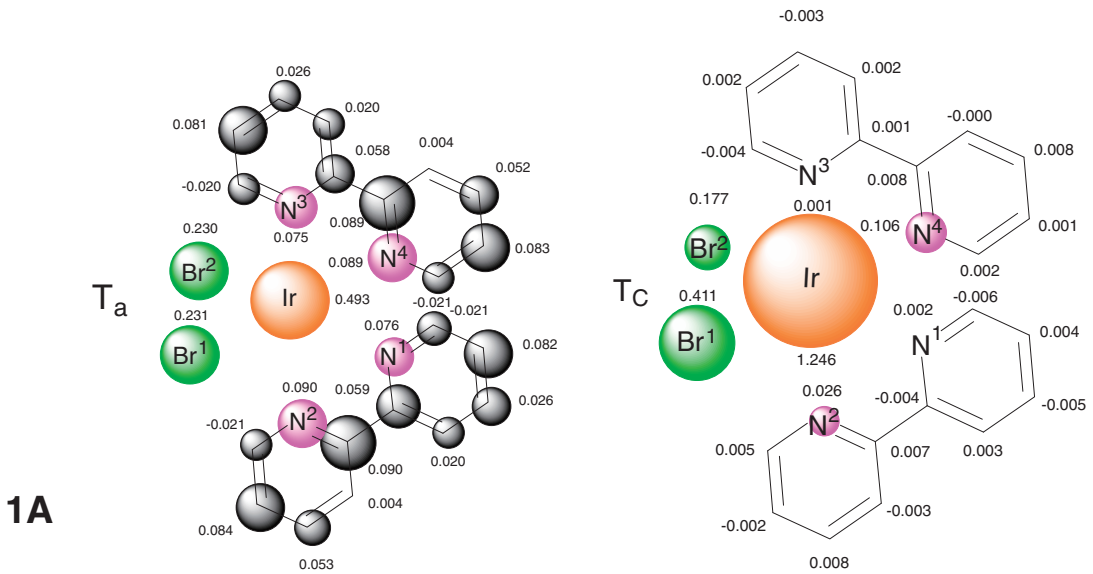

Figure 4. Mulliken spin densities of two triplet states (T_a and T_c) of complex **1A**. Sizes of circles represent the magnitude of the densities.

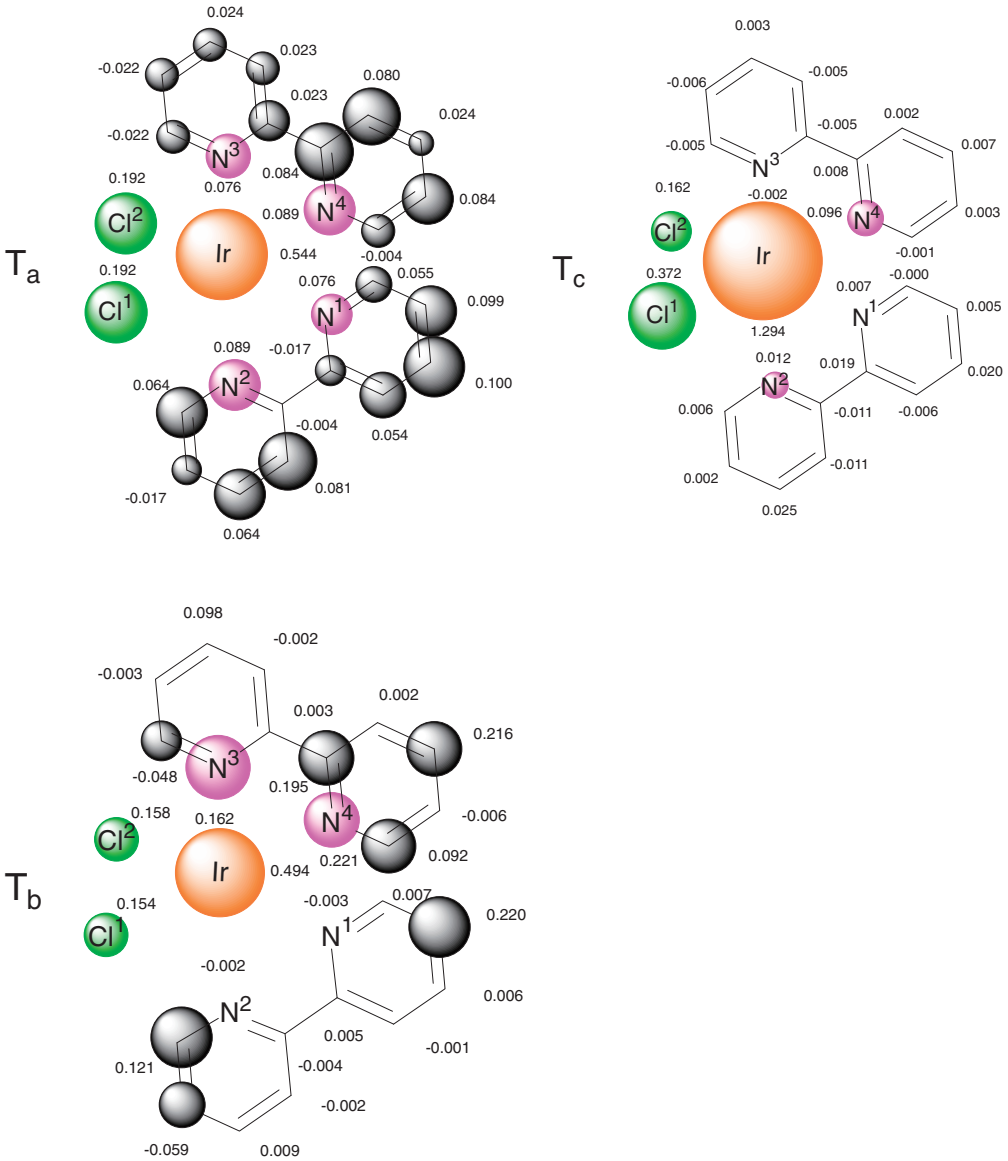

Figure 5. Mulliken spin densities of three triplet states (T_a, T_b, and T_c) of complex **1B**.

nonequivalent bpy and phen ligands through the pseudo-Jahn–Teller geometric distortion, respectively. The dichloro complexes with asymmetric spin density distributions (in T_b shown later in Figure 5) were thought to contribute to stronger emission spectra than those for the dibromo complexes.

Conclusion

Emission and electronic properties of eight iridium(III) polypyridine complexes containing two halide ions have been investigated experimentally and computationally. Particular interest has been paid to the similarity and difference between dibromo and dichloro complexes. Absorption spectra are similar between them. On the other hand, the dichloro complexes are better emitters than the dibromo compounds. In order to understand the difference, DFT calculations were carried out for complexes **1A**, **1B**, **3A**, and **3B**. Strikingly, for **1A** and **3A**, T_a and T_c were obtained whereas for **1B** and **3B**, T_a, T_b, and T_c. The ($T_a \rightarrow T_b$) conversion transition state (T_{ts}) could be successfully determined, where the activation energies (E_a's) are extremely small, e.g., $E_a(T_a \rightarrow T_{ts}) = +0.25\,\mathrm{kcal\,mol^{-1}}$ for complex **1B**. A clear contrast between dibromo and dichloro complexes was found in the destabilization energy (ΔE) relative to the ground state energy (Table 5). For the dichloro complex, $\Delta E(T_a)$ is nearly equal to $\Delta E(T_b)$ and also to the experimental energy, E_{em}. On the other hand, $\Delta E(T_c)$ is smaller than E_m. For the dibromo complex, $\Delta E(T_a) \approx E_{em} > \Delta E(T_c)$. Thus, the dibromo complex does not have the second emitter state of T_b, which inevitably gives weak radiative relaxation (Scheme 2).

Experimental

Reagents. Iridium(III) tribromide monohydrate ($IrBr_3 \cdot H_2O$), bpy, dmbpy, phen, dpphen, potassium hexafluorophosphate (KPF_6), and tetrabutylammonium perchlorate (TBAP) were purchased from Aldrich and used without further purification. Acetonitrile used in the spectroscopic and electrochemical measurements was of spectroscopic grade from Dojindo Laboratory. Syntheses of the complexes were undertaken by using a Mitsubishi Electric microwave oven (Model;

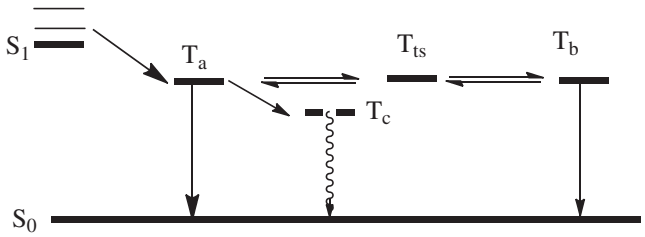

Scheme 2. T_a, T_b, and T_c are the structures of the triplet states. T_{ts} stands for the transition state for $T_a \rightarrow T_b$ interconversion.

RR-12AF; 500 W, 2450 MHz) on medium-high power in a round-bottom flask fitted with a reflux condenser.[10]

Syntheses of the Br^- Containing Complexes, 1A, 2A, 3A, and 4A. The desired complex $[IrBr_2(phen)_2]PF_6$ was prepared by a sequential procedure with a ligand replacement. For example, $IrBr_3 \cdot H_2O$ (0.5 mmol) and phen (0.180 g, 1.0 mmol) were mixed in ethylene glycol (15 mL). The suspended mixture was refluxed for 15 min in a microwave oven under a purging nitrogen atmosphere. Next, the mixture was cooled to room temperature. A saturated aqueous solution of KPF_6 (20 mL) was added as a counter ion, and a yellow product began to precipitate. Yellow single crystals were obtained by recrystallization from acetonitrile and water. The other iridium complexes were synthesized by the same procedure as in our previous work.[27,28]

$[IrBr_2(bpy)_2]PF_6$ (1A·PF_6^-): Yield 19% (80 mg), $C_{20}H_{16}N_4IrBr_2PF_6 \cdot H_2O$ (827.36): Calcd: C, 29.01; H, 2.18; N, 6.77%. Found: C, 28.52; H, 2.04; N, 6.37%. ^{1}H NMR (400 MHz, CD_3CN): δ 7.30 (dd, 2H, $J = 6.4$ Hz and 3.2 Hz), 7.57 (d, 2H, $J = 6.0$ Hz), 7.86 (dd, 2H, $J = 7.6$ Hz and 1.6 Hz), 7.97 (dd, 2H, $J = 6.0$ Hz and 2.8 Hz), 8.26 (dd, 2H, $J = 6.0$ Hz and 2.8 Hz), 8.34 (d, 2H, $J = 8.0$ Hz), 8.46 (d, 2H, $J = 8.8$ Hz), 9.91 (d, 2H, $J = 5.6$ Hz). ESI MS m/z 721.12 ($[M]^+$ requires 720.46). ESI MS m/z 585.24 ($[M - Br^- - H^+]^+$ requires 584.48).

$[IrBr_2(dmbpy)_2]PF_6$ (2A·PF_6^-): Yield 25% (110 mg), $C_{24}H_{24}N_4IrBr_2PF_6$ (865.43): Calcd: C, 33.31; H, 2.80; N, 6.47%. Found: C, 33.70; H, 2.78; N, 6.40%. ^{1}H NMR (400 MHz, CD_3CN): δ 7.58–7.83 (m, 4H), 8.02 (d, 2H, $J = 6.0$ Hz), 8.15 (d, 2H, $J = 9.2$ Hz), 8.29 (d, 2H, $J = 5.6$ Hz), 10.41 (d, 2H, $J = 5.6$ Hz). ESI MS m/z 721.12 ($[M]^+$ requires 720.46).

$[IrBr_2(phen)_2]PF_6$ (3A·PF_6^-): Yield 18% (75 mg), $C_{24}H_{16}N_4IrBr_2PF_6$ (857.41): Calcd: C, 33.62; H, 1.88; N, 6.53%. Found: C, 33.82; H, 1.98; N, 6.60%. ^{1}H NMR (400 MHz, CD_3CN): δ 7.56 (dd, 2H, $J = 8.0$ Hz and 2.0 Hz), 7.82 (d, 2H, $J = 5.2$ Hz), 8.24 (d, 2H, $J = 8.8$ Hz), 8.30–8.36 (m, 4H), 8.55 (d, 2H, $J = 8.0$ Hz), 8.93 (d, 2H, $J = 8.0$ Hz), 10.28 (d, 2H, $J = 5.6$ Hz). ESI MS m/z 713.02 ($[M]^+$ requires 712.45).

$[IrBr_2(dpphen)_2]PF_6$ (4A·PF_6^-): Yield 21% (120 mg), $C_{48}H_{32}N_4IrBr_2PF_6$ (1161.80): Calcd: C, 49.62; H, 2.78; N, 4.82%. Found: C, 49.75; H, 2.78; N, 5.23%. ^{1}H NMR (400 MHz, CD_3CN): δ 7.21 (d, 2H, $J = 4.8$ Hz), 7.43 (d, 2H, $J = 5.6$ Hz), 7.75 (dd, 2H, $J = 9.2$ Hz and 5.6 Hz), 8.24 (m, 4H), 8.35 (m, 4H), 9.75 (d, 2H, $J = 5.6$ Hz). ESI MS m/z 1017.27 ($[M]^+$ requires 1016.84).

The corresponding Cl^- containing complexes of **1B**, **2B**, **3B**, and **4B** have been reported previously.[10]

Measurements. Electronic absorption spectra of **1A**, **2A**, **3A**, and **4A** were recorded at room temperature in CH_3CN solution with a Shimadzu UV-2550 spectrophotometer. ESI-MS spectra were obtained with a JEOL JMS-T100LC AccuTOF spectrometer. Cyclic voltammetries (CVs) were measured on an ALS-610B electrochemical analyzer fitted with a three-electrode system consisting of a glassy carbon working electrode, a platinum auxiliary electrode, and an Ag/AgCl reference electrode. CV experiments were performed for AN solutions of the complexes (5.0×10^{-4} M) and 0.050 M TBAP under nitrogen atmosphere at 25 °C with a scan rate of 100 mV s^{-1}. The emission lifetimes were measured in N_2-saturated CH_3CN solutions using a Horiba TemPro fluorescence lifetime system with an excitation by NanoLED. The emission quantum yields for the iridium complexes were determined in CH_3CN at room temperature relative to those of a solution containing $[Ru(bpy)_3]Cl_2$ ($\Phi = 0.095$)[29] and having the same absorbance at the excitation wavelength.

Crystallographic Data Collection and Structure Determination of 3A. The measurements were made on a Rigaku R-Axis-Rapid Imaging Plate diffractometer with graphite monochromated Mo Kα radiation (Table S1). Indexing was performed from 3 oscillations. The camera radius was 127.40 mm. Readout was performed in the 0.100 mm pixel mode. The structures were solved by direct methods and were refined on F^2 by full-matrix least-squares methods, using SHELXL-97.[30] The non-hydrogen atoms were refined anisotropically by the full-matrix least-squares method. All hydrogen atoms were isotropically refined. CCDC 797043 contains the supplementary crystallographic data for this paper. These data can be obtained free of charge from the Cambridge Crystallographic Data Centre via www.ccdc.cam.ac.uk/data_request/cif.

Computational Methods. DFT calculations of the four complexes **1A**, **1B**, **3A**, and **3B** were performed using the Gaussian98 program package.[31] The Becke three parameters hybrid exchange and the Lee–Yang–Parr correlation functionals (B3LYP) were used.[32,33] Geometries in the singlet closed-shell and triplet states were fully optimized by the R(U)B3LYP method. The transition-state (TS) geometry was determined in the following way. First, the geometries of the two different triplet states (T_a and T_b) were obtained. Second, the intermediate geometry between T_a and T_b was constructed and it was used as an initial geometry for the partial optimization with the fixed distances of C5–C6 and C17–C18. Third, by the use of the Hessian matrix (i.e., the second derivative of the total electronic energy) stored in the partial optimization, the TS geometry was sought. The spin contaminations in the triplet state are safely small, e.g., $\langle S^2 \rangle = 2.007$, for the triplet state T_a of complex **1A**. In the basis set (LANL2DZ)[34] (6-311+G(d)[35]), LANL2DZ was used for the Ir^{3+} metal and 6-311+G(d) was used for other atoms.

Supporting Information

The ORTEP of **3A**, mulliken spin densities of complexes **3A** and **3B**, crystallographic data of complex **3A**, cartesian coordinates of the optimized geometries, and calculated data of singlet, T_a, T_c, and T_{ts}. This material is available free of charge on the web at http://www.csj.jp/journals/bcsj/.

References

1 E. Baranoff, J.-H. Yum, M. Graetzel, Md. K. Nazeeruddin, *J. Organomet. Chem.* **2009**, *694*, 2661.

2 A. J. Wilkinson, A. E. Goeta, C. E. Foster, J. A. G. Williams, *Inorg. Chem.* **2004**, *43*, 6513.

3 K. Dedeian, J. Shi, N. Shepherd, E. Forsythe, D. C. Morton, *Inorg. Chem.* **2005**, *44*, 4445.

4 A. Auffrant, A. Barbieri, F. Barigelletti, J.-P. Collin, L. Flamigni, C. Sabatini, J.-P. Sauvage, *Inorg. Chem.* **2006**, *45*, 10990.

5 J. D. Slinker, J. Rivnay, J. S. Moskowitz, J. B. Parker, S. Bernhard, H. D. Abruña, G. G. Malliaras, *J. Mater. Chem.* **2007**, *17*, 2976.

6 M. A. Baldo, S. Lamansky, P. E. Burrows, M. E. Thompson, S. R. Forrest, *Appl. Phys. Lett.* **1999**, *75*, 4.

7 M. S. Lowry, S. Bernhard, *Chem.—Eur. J.* **2006**, *12*, 7970.

8 C. Ulbricht, B. Beyer, C. Friebe, A. Winter, U. S. Schubert, *Adv. Mater.* **2009**, *21*, 4418.

9 J. Slinker, D. Bernards, P. L. Houston, H. D. Abruña, S. Bernhard, G. G. Malliaras, *Chem. Commun.* **2003**, 2392.

10 N. Yoshikawa, J. Sakamoto, T. Matsumura-Inoue, H. Takashima, K. Tsukahara, N. Kanehisa, Y. Kai, *Anal. Sci.* **2004**, *20*, 711.

11 R. Terki, L.-P. Simoneau, A. Rochefort, *J. Phys. Chem. A* **2009**, *113*, 534.

12 B. Minaev, V. Minaeva, H. Ågren, *J. Phys. Chem. A* **2009**, *113*, 726.

13 F. J. Coughlin, M. S. Westrol, K. D. Oyler, N. Byrne, C. Kraml, E. Zysman-Colman, M. S. Lowry, S. Bernhard, *Inorg. Chem.* **2008**, *47*, 2039.

14 S. Stagni, S. Colella, A. Palazzi, G. Valenti, S. Zacchini, F. Paolucci, M. Marcaccio, R. Q. Albuquerque, L. De Cola, *Inorg. Chem.* **2008**, *47*, 10509.

15 M. Bandini, M. Bianchi, G. Valenti, F. Piccinelli, F. Paolucci, M. Monari, A. Umani-Ronchi, M. Marcaccio, *Inorg. Chem.* **2010**, *49*, 1439.

16 Md. Nazeeruddin, R. T. Wegh, Z. Zhou, C. Klein, Q. Wang, F. De Angelis, S. Fantacci, M. Grätzel, *Inorg. Chem.* **2006**, *45*, 9245.

17 F. De Angelis, S. Fantacci, N. Evans, C. Klein, S. M. Zakeeruddin, J.-E. Moser, K. Kalyanasundaram, H. Bolink, M. Grätzel, M. K. Nazeeruddin, *Inorg. Chem.* **2007**, *46*, 5989.

18 D. Di Censo, S. Fantacci, F. De Angelis, C. Klein, N. Evans, K. Kalyanasundaram, H. J. Bolink, M. Grätzel, M. K. Nazeeruddin, *Inorg. Chem.* **2008**, *47*, 980.

19 B. Divisia, P. C. Ford, R. J. Watts, *J. Am. Chem. Soc.* **1980**, *102*, 7264.

20 L. Yang, F. Okuda, K. Kobayashi, K. Nozaki, Y. Tanabe, Y. Ishii, M.-a. Haga, *Inorg. Chem.* **2008**, *47*, 7154.

21 T. Sajoto, P. I. Djurovich, A. B. Tamayo, J. Oxgaard, W. A. Goddard, III, M. E. Thompson, *J. Am. Chem. Soc.* **2009**, *131*, 9813.

22 T. Hofbeck, H. Yersin, *Inorg. Chem.* **2010**, *49*, 9290.

23 H. Yersin, *Transition Metal and Rare Earth Compounds Excited States, Transitions, Interactions III* in *Topics in Current Chemistry*, ed. by H. Yersin, Springer-Verlag, Berlin, **2004**, Vol. 241, pp. 1–26. doi:10.1007/b96858.

24 H. Yersin, D. Donges, *Transition Metal and Rare Earth Compounds Excited States, Transitions, Interactions II* in *Topics in Current Chemistry*, ed. by H. Yersin, Springer-Verlag, Berlin, **2001**, Vol. 214, pp. 81–186. doi:10.1007/3-540-44474-2_3.

25 H. Yersin, W. Humbs, J. Strasser, *Electronic and Vibronic Spectra of Transition Metal Complexes II* in *Topics in Current Chemistry*, ed. by H. Yersin, Springer-Verlag, Berlin, **1997**, Vol. 191, pp. 153–249. doi:10.1007/BFb0119213.

26 H. Yersin, W. Humbs, J. Strasser, *Coord. Chem. Rev.* **1997**, *159*, 325.

27 N. Yoshikawa, S. Yamabe, N. Kanehisa, Y. Kai, H. Takashima, K. Tsukahara, *Eur. J. Inorg. Chem.* **2007**, 1911.

28 N. Yoshikawa, S. Yamabe, N. Kanehisa, Y. Kai, H. Takashima, K. Tsukahara, *Inorg. Chim. Acta* **2006**, *359*, 4585.

29 K. Suzuki, A. Kobayashi, S. Kaneko, K. Takehira, T. Yoshihara, H. Ishida, Y. Shiina, S. Oishi, S. Tobita, *Phys. Chem. Chem. Phys.* **2009**, *11*, 9850.

30 G. M. Sheldrick, *SHELXL 97*, University of Göttingen, Germany, **1997**.

31 M. J. Frisch, G. W. Trucks, H. B. Schlegel, G. E. Scuseria, M. A. Robb, J. R. Cheeseman, V. G. Zakrzewski, J. A. Montgomery, Jr., R. E. Stratmann, J. C. Burant, S. Dapprich, J. M. Millam, A. D. Daniels, K. N. Kudin, M. C. Strain, O. Farkas, J. Tomasi, V. Barone, M. Cossi, R. Cammi, B. Mennucci, C. Pomelli, C. Adamo, S. Clifford, J. Ochterski, G. A. Petersson, P. Y. Ayala, Q. Cui, K. Morokuma, D. K. Malick, A. D. Rabuck, K. Raghavachari, J. B. Foresman, J. Cioslowski, J. V. Ortiz, A. G. Baboul, B. B. Stefanov, G. Liu, A. Liashenko, P. Piskorz, I. Komaromi, R. Gomperts, R. L. Martin, D. J. Fox, T. Keith, M. A. Al-Laham, C. Y. Peng, A. Nanayakkara, C. Gonzalez, M. Challacombe, P. M. W. Gill, B. Johnson, W. Chen, M. W. Wong, J. L. Andres, C. Gonzalez, M. Head-Gordon, E. S. Replogle, J. A. Pople, *Gaussian 98 (Revision A.7)*, Gaussian Inc., Pittsburgh PA, USA, **1998**.

32 C. Lee, W. Yang, R. G. Parr, *Phys. Rev. B* **1988**, *37*, 785.

33 A. D. Becke, *J. Chem. Phys.* **1993**, *98*, 5648.

34 P. J. Hay, W. R. Wadt, *J. Chem. Phys.* **1985**, *82*, 299.

35 M. M. Francl, W. J. Pietro, W. J. Hehre, J. S. Binkley, M. S. Gordon, D. J. DeFrees, J. A. Pople, *J. Chem. Phys.* **1982**, *77*, 3654.